Middle Holocene palaeoflood extremes of the Lower Rhine

Willem H. J. Toonen, Michiel M. de Molenaar, Frans P. M. Bunnik and Hans Middelkoop

ABSTRACT

A Chézy-based hydraulic model was run to estimate the magnitude of extreme floods of Middle Holocene age in the Lower Rhine Valley (Germany). Input parameters were gathered from the field and literature, and used in ten scenarios to calculate a best guess estimate for the minimum size of extreme floods. These events have been registered as slackwater deposits on elevated terrace levels and in a palaeochannel fill. The modelled minimum discharge is 13,250 m^3 sec^{-1} for a Middle Holocene flood with an estimated recurrence interval between 1,250 and 2,500 years. A sensitivity analysis on different input parameters enables evaluation of factors which cause the relatively large range in modelled discharges. Understanding the origin of uncertainties in modelled discharges is important for making geologically based calculations of palaeoflood magnitudes important in modern flood frequency analyses, which generally lack information on the magnitudes of rare events.

Key words | exceedance boundary, flood frequency analysis, Lower Rhine, palaeoflood, palaeostage indicators

Willem H. J. Toonen (corresponding author)
Michiel M. de Molenaar
Hans Middelkoop
Department of Physical Geography,
Utrecht University,
Utrecht,
The Netherlands
E-mail: *W.H.J.Toonen@uu.nl*

Willem H. J. Toonen
Department of Applied Geology and Geophysics,
Deltares BGS,
Utrecht,
The Netherlands

Frans P. M. Bunnik
TNO, Geological Survey of The Netherlands,
Utrecht,
The Netherlands

INTRODUCTION

Flood safety assessment for the Lower Rhine in the Netherlands and Germany demands insight into the recurrence interval and magnitude of extreme events. Flood safety legislation in the Netherlands is based on the discharge of the 1/1,250-yr flood. The actual size of this statistical magnitude needs to be specified, as it is used in the design and maintenance of dikes in the Rhine delta (The Netherlands). Current practice is to calculate the design flood (Q_{1250}) by statistical extrapolation from an observational flood series that covers the 20th century, which is too short for an accurate estimation of extreme events. The inclusion of the relatively large 1993 and 1995 floods in this series in a recalculation 16 years ago raised the projected size of Q_{1250} from ~15,000 to ~16,000 m^3 s^{-1} (Chbab 1996). This demanded extra financial investment and altered land use planning for embanked floodplains to maintain the present-day safety standards. Furthermore, in the anticipated future climate the Q_{1250} is expected to rise by 10–15% (Kwadijk & Middelkoop 1994; Shabalova *et al.* 2003), which increases the need to reduce uncertainty in the prediction of Q_{1250}. The 95% confidence interval for the current estimate of Q_{1250} stretches from 13,220 to 18,630 m^3 s^{-1} (Chbab *et al.* 2006). To narrow this interval and to quantify Q_{1250} as precisely as possible, methods other than statistical extrapolation of gauged observations of the last ~110 years should be investigated.

It is likely that Q_{1250} exceeds the largest flood of the Rhine observed in the last century (Lobith, Figure 1; ~12,600 m^3 s^{-1} in AD 1926). Herget & Euler (2010) clearly illustrate that since AD ~ 1300 at least five Rhine floods were larger than the 1993 and 1995 floods at Cologne (Germany), of which two (AD 1374 and 1651) probably had discharges comparable with or higher than the current design flood. Constraining the magnitudes of extreme

doi: 10.2166/nh.2012.162

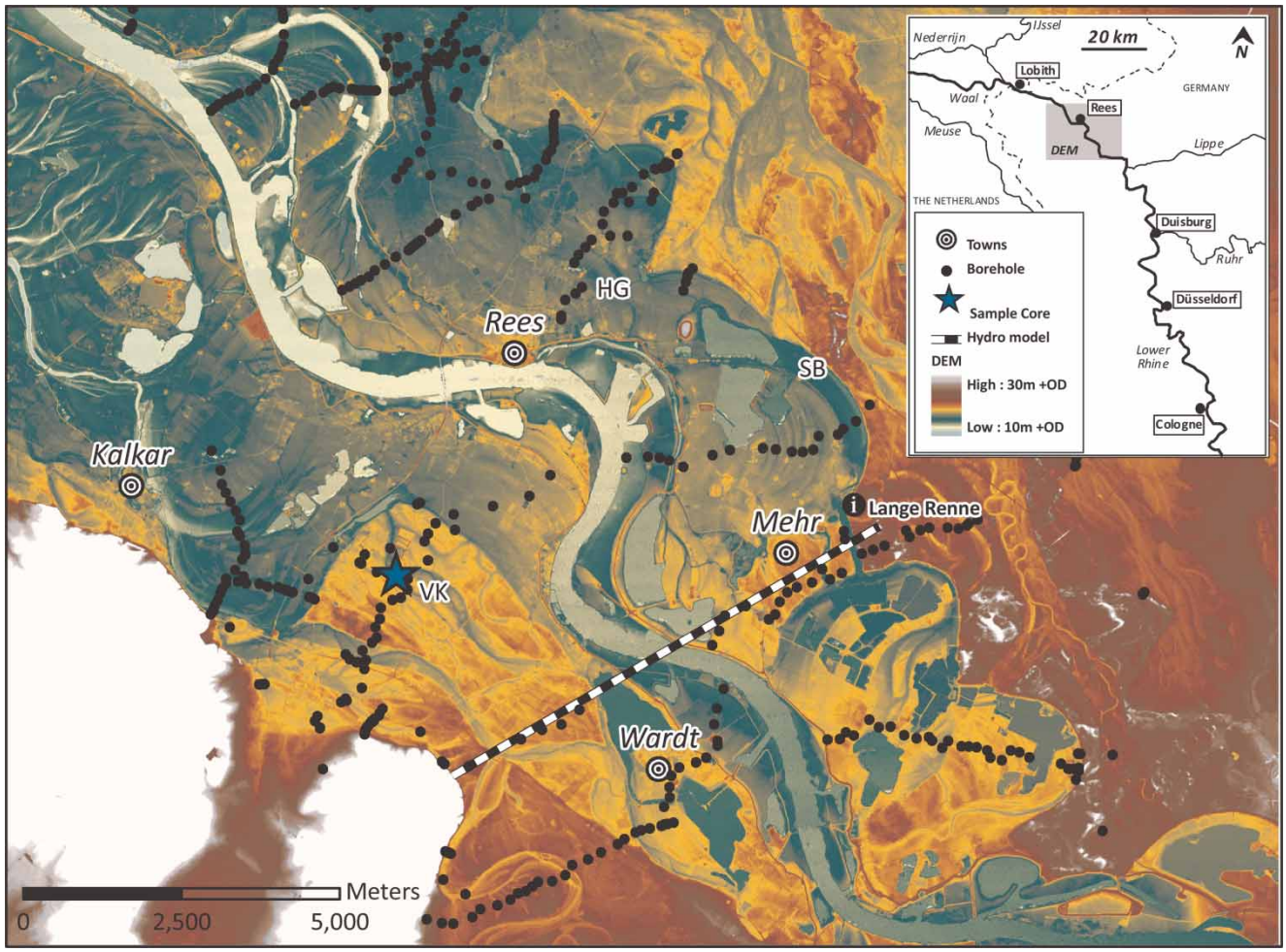

Figure 1 | DEM of the Lower Rhine research area with location of the model transect, boreholes, the Vossekuhl (VK) sample core, and the Middle Holocene palaeochannels 'Schloss Bellinghoven' (SB) and 'Haus Groin' (HG).

palaeofloods (here defined as floods with a recurrence time larger than 1,000 years) may significantly improve the outcomes of flood frequency analysis. Their magnitude can be estimated using a combination of geological evidence and palaeohydrological calculations (Benito *et al.* 2004; Herget *et al.* 2013). In this paper, we assess palaeoflood magnitudes associated with sedimentary palaeostage indicators of Middle Holocene age in the Lower Rhine Valley, downstream of the last main tributary, with the goal of constraining the lower limits of the Q_{1250} flood.

Palaeohydrological estimates of extreme discharges (e.g., Baker 1987; Baker *et al.* 2002) have larger uncertainties in reconstructed magnitude and recurrence interval than gauged records of more moderate flows. Nevertheless, results are often suitable to 'bracket what is physically possible' (Redmond *et al.* 2002). They can be used to create flood envelopes between lower estimates of palaeoflood discharges and upper non-exceedance limits (Levish 2002; O'Connell *et al.* 2002). This constrains statistical flood frequency-magnitude extrapolations between limits in the reach that lie beyond the recurrence times of moderately sized gauged floods.

In this study, a palaeohydrological lower limit for Q_{1250} is reported, based on highest Middle Holocene palaeoflood markers. Observations were derived from a time when the Lower Rhine Valley and its hinterland were still largely naturally forested, but with a similar fluvial style as in the human-influenced Late Holocene. In the Middle Holocene, the Lower Rhine reached its maximum incision before Late Holocene aggradation initiated (Erkens *et al.* 2011), so only

extreme floods with a large amplitude could leave deposits on the elevated terraces flanking the valley. These rare depositional events are more easily traced and have been better preserved in the local depressions on the elevated terraces (such as organically infilled palaeochannels, abandoned in the Early Holocene) than Late Holocene deposits of individual floods, which are difficult to distinguish among common overbank deposits of that period. Moreover, Late Holocene deposits on elevated terraces are near or at the surface, making them highly vulnerable to post-depositional disturbance by bioturbation and ploughing.

For a selected transect across the Lower Rhine Valley (Germany; Figure 1), a Chézy-based hydraulic cross-section model was set up using carefully selected geological data: Middle Holocene channel dimensions, surrounding floodplain landscape, surface roughness (channel bed and vegetation) and palaeostage indicators (water level proxies). In multiple scenarios, set-up parameters were varied within realistic limits to explore the range of discharges and as a means of sensitivity analysis. First, the hydraulic model is described, with an explanation of the input data and their value range used in different model scenarios. Second, the range in discharge outcomes is discussed, with the focus on the origin of uncertainties and the contribution of different input variables. Last, the utilization of these data is discussed: i.e., how should one use these model results in *modern* flood frequency analysis?

PALAEOFLOOD RECONSTRUCTION METHODOLOGY

Hydraulic radius (wetted cross-section), slope and surface roughness are the main inputs for the calculation of the palaeoflood discharge in a valley-wide transect. These all depend on the characteristics of the palaeolandscape. The palaeotopography was reconstructed starting with a Digital Elevation Model (DEM; Lidar-based 10×10 m grid, sub-decimetre vertical resolution, filtered vegetation and urban areas; Landvermessungsamt Nordrhein-Westfalen, Germany; as used in Cohen *et al.* (2009)). Elevation of the present surface was sampled every 10 metres along the 13.3-km long transect (Figure 1). An extensive handcoring programme (34 in the transect, 232 in region) provided geological information to correct modern surface elevation to the palaeosurface for the Middle Holocene situation. Later deposits were removed based on extensive lithological mapping, cross-cutting relationships of deposits and the existing chronology of deposits, which has been established in previous studies with radiocarbon, OSL and archaeological dating (Klostermann 1992; Erkens *et al.* 2011). Coring and mapping methods for the floodplain deposits and palaeochannel geometries are described in Erkens *et al.* (2011) and Toonen *et al.* (2012), respectively.

To minimize uncertainty in palaeohydrological calculations, a section along the Lower Rhine was chosen where the position of the main channel has changed relatively little since the Middle Holocene (Figures 1–3). A relatively large part of this section is characterized by higher terrace levels, which have rarely experienced Middle Holocene flooding (Klostermann 1992). This choice minimizes uncertainty in several calculation inputs; it secures the availability of sites that record palaeostage indicators (PSIs) for the highest floods only and it reduces the number of options for palaeochannel bedmorphology (discussed below). The multiple terrace steps in the terrain combined with the presence of PSIs in residual channels provide excellent constraints on the water levels during floods (Figures 1–3). The residual

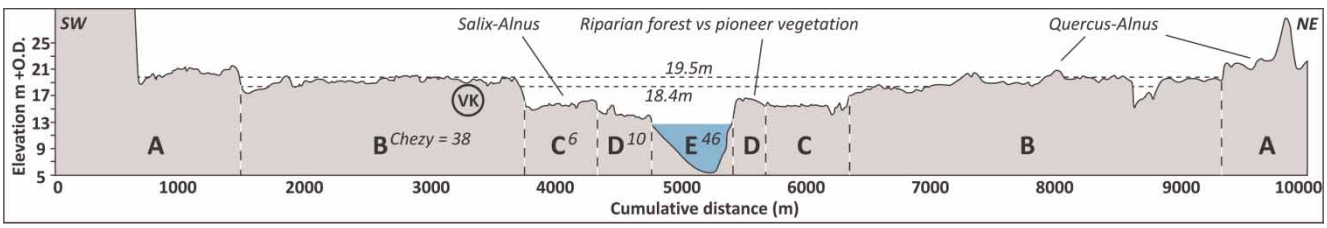

Figure 2 | Modelled valley cross-section with classification per floodplain compartment with general vegetation composition, the projected location of the Vossekuhl (VK) sample core, upper and lower estimated water levels, and zone-averaged Chézy roughness values for the best guess estimate (BGE). Parameter values for bed slope and vegetation are shown in Table 2.

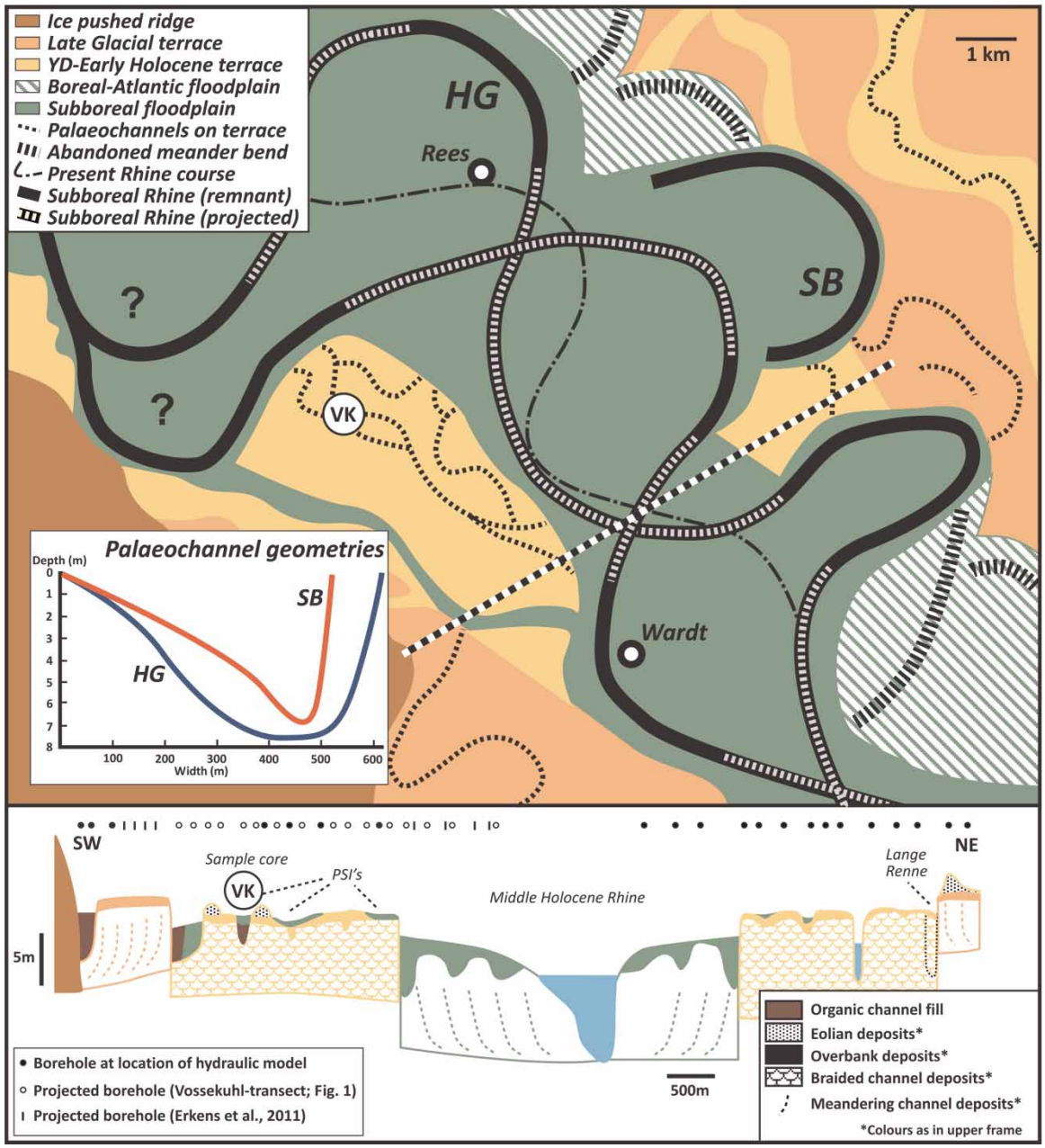

Figure 3 | Reconstruction of the Middle Holocene Lower Rhine Valley with Subboreal Rhine courses and older morphology (after Klostermann 1992; Erkens *et al*. 2011; Geurts 2011; Van Munster 2011). YD = Younger Dryas. The inset shows palaeochannel dimensions of the Schloss Bellinghoven (SB) and Haus Groin (HG) palaeochannels, which have been used as variables in model scenario 4. A schematized geological cross-section is shown in the lower frame (modified after Erkens *et al*. 2011; Geurts 2011). VK = projected Vossekuhl sample core location.

channels on the high levels provide (1) registration of the minimum water level during extreme flooding events (occasional clay intercalations in dominantly organic channel fills), (2) constraints on the timing and recurrence interval of such an event (encased in easily datable, non-reworked material) and (3) indicative means to reconstruct past floodplain vegetation out of the preserved fossil pollen assemblages. Palynological analyses indicate a widely forested floodplain at the beginning of the Subboreal period, which is in agreement with existing archaeological

insights in timing and propagation of agricultural revolutions (i.e., Neolithic to Bronze Age transition; e.g., Lechner 2009) and palaeogeographical insights in the impact thereof on the Lower Rhine (e.g., Erkens *et al.* 2011). The recurrence intervals of the PSI-producing floods are estimated from acceleration mass spectrometry (AMS) dating and palynological analysis of the channel fill deposits.

Discharge calculations

Palaeoflood discharges were calculated with Chézy-based formulas, following a slope–area approach on a single transect (cf. Dalrymple & Benson 1968). The transect was divided into five floodplain compartments (Figure 2), because conditions may vary significantly over a submerged floodplain during floods. Input values for hydraulic radius, slope and roughness were gathered from the field and literature to estimate values for five floodplain compartments separately. Compartments were based on terrace topography, elevation above the reconstructed Middle Holocene floodplain and associated vegetation type.

The standard Chézy-formula (Equation (1)) was used to calculate mean flow velocities that occurred during the flood stage reconstructed from the PSIs. Open channel roughness values (Zone E; Figure 2) were calculated using Equation (2) (Keulegan 1938; Van Rijn 1984). Equation (3) was used for densely vegetated floodplain compartments where surface roughness is determined by (partially) submerged vegetation, and where the effect of bed friction can be neglected (Baptist *et al.* 2007). In the case of partially submerged vegetation, only the first part of Equation (3) is used, and vegetation height (k) is replaced by water depth (h). This formulation for the Chézy-roughness over flooded vegetated floodplain compartments is derived from parameterized semi-natural vegetation plots (Keijzer *et al.* 2005; Baptist *et al.* 2007) (and is the main reason for applying Chézy instead of other methods to estimate roughness). In Equation (3), $m*D*k$ can be substituted with Ar (representative stem surface; $m^2m^{-2}m^{-1}$), to calculate roughness in forested areas. Cross-sectional area and flow velocity were calculated per 10-m interval in the cross-section and their products are summed to obtain the total discharge.

$$\bar{u} = C\sqrt{Ri} \tag{1}$$

$$C = 18\log\frac{12h}{k_s} \tag{2}$$

$$C = \sqrt{\frac{2g}{C_D m D k}} + 2\sqrt{g}\ln\left(\frac{h}{k}\right) \tag{3}$$

where $\bar{u}$ = depth-averaged velocity ($m\,s^{-1}$), C = Chézy coefficient ($m^{1/2}\,s^{-1}$), R = hydraulic radius (m), i = water level slope, k_s = sand roughness of Nikuradse (m; Keulegan 1938), g = gravitational acceleration (9.81 $m\,s^{-2}$), C_D = bulk drag coefficient, m = number of vegetation stems per m^2 horizontal surface area, D = vegetation stem diameter (m), h = water depth (m), and k = vegetation height (m).

Model parameters and scenarios

For ten input parameters we selected a range based on literature, local geological data and personal observations (Table 1). This results in a spread of outcomes in palaeodischarge calculated for these parameters. In 18 different model runs, the range (minimum and maximum estimate) and best guess estimate (BGE) of each parameter were used to evaluate the discharge response to individually changing parameters. These minimum and maximum values for the input parameters were aimed at: (1) estimating a realistic minimum flood discharge; and (2) assessing the uncertainty in discharge outcomes that results from the range in geologically derived input parameters. Our BGE aims to provide a specific lower limit for flood magnitude in flood frequency analysis.

Water depth

The water depth is here defined as the difference between palaeotopographical level in each subsection and the water level during floods reconstructed from PSIs. To reconstruct the palaeotopography, elevation artefacts were removed first. Artificially raised areas such as dikes,

Table 1 | Overview of model input parameters with associated scenario, parameter range and data sources

Model parameter	Factor	Scenario description	Range MIN	BGE	MAX	Source
Hydraulic radius	Palaeotopography	1. Removal of Lange Renne bypass channel.	Complete	Complete	Replacement	Borehole data; DEM; Erkens *et al.* (2011)
		2. Stripping of overbank deposition on Early Holocene terraces.	None	None	0.3 m	
		3. Stripping of Late Holocene sedimentation of Middle Holocene floodplain (Zones C + D; Figure 2).	1 m	1.3 m	1.8 m	
		4. Palaeochannel dimensions SB/HG (Figure 3).	SB	HG	HG	
	Palaeostage indicator	5. PSI in palaeochannel fill, Early Holocene terraces, and non-exceedence boundaries (Figure 1).	18.4 m +OD	18.4 m +OD	19.5 m +OD	
Slopes	Bed slope	6. Local and regional slopes of floodplain levels.	Table 2; data displayed per floodplain compartment.			Erkens *et al.* (2011); Van Munster (2011)
		7. Sinuosity of palaeochannels.	$\Phi = 1.5$	$\Phi = 1.3$	$\Phi = 1.2$	Palaeo-reconstruction (Figure 3)
Roughness	Bed	8. Grain size in thalweg deposits of palaeochannel fill, estimated dune heights and channel bed roughness during floods.	$ks = 0.5$	$ks = 0.3$	$ks = 0.15$	Borehole data; Hesselink & Kleinhans (2002); Wilbers & ten Brinke (2003); Frings & Kleinhans (2008)
	Vegetation	9. Vegetation composition ratios (climax vs pioneer; on lower floodplain compartment only; Table 2).	$C = 5:1$	$C = 4:1$	$C = 2:1$	Wolf *et al.* (2001); Van Velzen *et al.* (2002a, 2002b); Field observations; palynological analyses
		10. Density and maturity of vegetation type.	Table 2; data displayed per floodplain compartment.			

elevated roads and urbanized areas were removed. Gravel pits were restored to the surrounding levels of the undisturbed floodplain. These changes were fixed in the model and do not vary between scenarios. Correction of modern elevations for natural changes due to channel migration and overbank sedimentation is less straightforward, and was therefore varied between scenarios. This also goes for removing or reconstructing artificial channels in the floodplain, in particular the 'Lange Renne' (Figure 1). As no documentation exists regarding the origin of this channel – it may be an entirely dug channel or a modified residual channel – the transect may either be corrected to surrounding terrace topography or be replaced by a previously existing palaeochannel. Because a palaeochannel may carry an important amount of discharge during high-water events, scenario 1 was used (Table 1) to evaluate differences in discharge outcomes during standard terrace topography (no channel), and by introducing a copy of

Table 2 | Scenario parameters for slope and specific vegetation for the different floodplain compartments (shown in Figure 2)

		Slope (*10^{-5} = cm/km)			Vegetation (C_D*Ar) or ($C_D^*$$m$*$D$*$k$)		
Compartment (Figure 2)	**Description**	**MIN**	**BGE**	**MAX**	**MIN**	**BGE**	**MAX**
A	LG terrace	21	22.5	27	1.5*0.13	1.5*0.05	1.5*0.023
B	YD-EH terrace	21	22.5	27	1.5*0.13	1.5*0.05	1.5*0.023
C	MH floodplain	17	18	22.5	1.5*0.13	1.5*0.05	1.5*0.023
D	Levee zone; mixed vegetation	17	18	22.5	1.5*0.13 1.8*140*0.003*0.2	1.5*0.05 1.8*100*0.003*0.2	1.5*0.023 1.8*50*0.003*0.2
E	Channel	17	18	22.5	–	–	–

LG = Late Glacial; YD = Younger Dryas; EH, MH = Early, Middle Holocene.

the nearby palaeochannel on the same terrace level (Figure 1).

In the following step, Late Holocene clay cover was stripped from lower parts of elevated terrace levels (Younger Dryas–Early Holocene; Figure 3), palaeochannel fills and the Middle Holocene floodplain. On pre-Holocene terrace levels, the topsoil consists of fine overbank deposits of Early Holocene age (Erkens *et al.* 2011), which have not been removed as they were already deposited prior to the investigated period. However, palaeochannel fills (which are depressions in the same terrace levels) hold Rhine deposits of Late Holocene age. This indicates that in our modelled cross-section, renewed floodplain aggradation may also have occurred outside the palaeochannels on top of Early Holocene terraces since the Iron Age (Figure 4). Due to extensive ploughing, the contribution of younger aggradation is difficult to distinguish from earlier deposits, as palaeosols have been destroyed and the coarser Late Holocene overbanks have become admixed with the typically denser and finer Early Holocene deposits (Erkens *et al.* 2011). The thickness of the Late Holocene overbanks is estimated to be 0.3 m at maximum, as this is the depth of plough horizon (scenario 2; Table 1). Late Holocene aggradation on the lower floodplain (scenario 3) was stripped using data from boreholes (this research and Erkens *et al.* 2011); the thickness varies between 1.0 and 1.8 m (generally around 1.3 m).

The shape of the present day Rhine channel is different from the Middle Holocene channel. The Rhine channel has shown natural morphological responses to changes in discharge and sediment load owing to deforestation of the floodplain and hinterland (Lang *et al.* 2003; Hoffmann *et al.* 2007; Erkens *et al.* 2011), and human modifications of the channel for navigation purposes and flood mitigation (Lammersen *et al.* 2002). In the transect, the modern Rhine channel is replaced by channel bed morphologies reconstructed from palaeochannel deposits (following Toonen *et al.* 2012) a few kilometres downstream of our section (Figure 3). These palaeochannels are of varying size and geometry, but typically wider, shallower and more sinuous than the present Rhine. The wider 'Haus Groin' (HG) palaeochannel serves as our BGE for the palaeochannel shape. It is considered most representative for a channel traversing the 'bottleneck' between older terraces where our transect is located (Figure 3). The narrower and more sinuous 'Schloss Bellinghoven' (SB) channel would be an alternative (that results in a lower discharge estimate; scenario 4), but the palaeogeographical situation limits the fit of such a sinuous channel with a very wide point bar through the modelled cross-section (Figures 1 and 3).

Constraints on the water level during palaeofloods were obtained from PSIs in channel fills and on different terrace levels (Figures 1–3). Collected PSIs (both clay deposition and non-exceedance boundaries) from the highest flooded terrace levels in the transect and immediately downstream of it, were corrected for the regional valley slope to create lower and upper limits of possible water levels. Deposition of clays on the lower parts of the Early Holocene terrace levels and in palaeochannel fills indicates a minimum flood water level of 18.4 m +OD (Amsterdam Ordnance Datum (NAP) = approximately mean sea level; Figure 2). Non-exceedance boundaries on higher elevated terraces and in more elevated palaeochannel fills constrain the maximum water level above these deposits to 19.5 m +OD

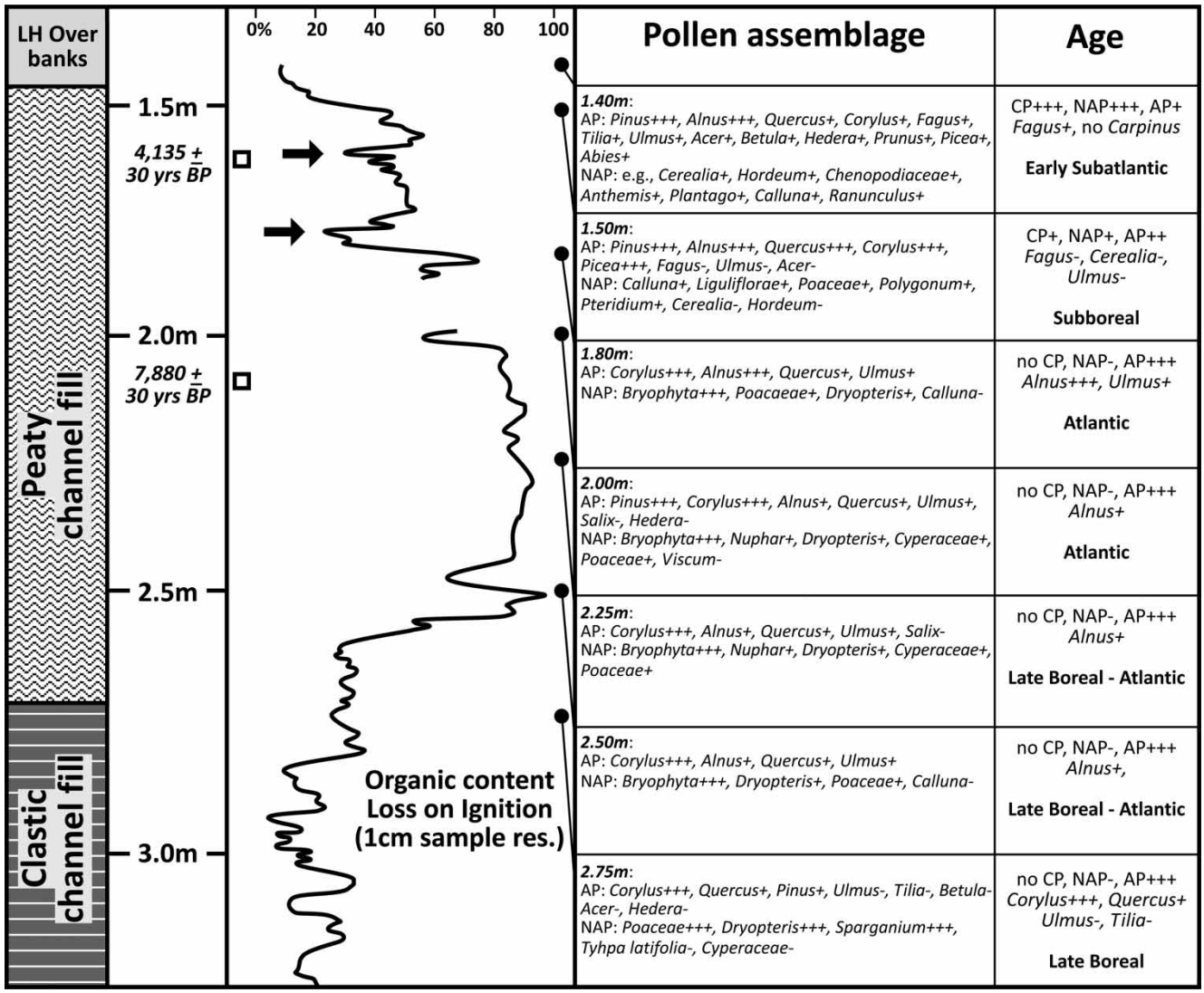

Figure 4 | The Vossekuhl sample core with general lithology, organic content, pollen assemblages and estimated ages (CP = culture crops pollen, NAP = non-arboreal pollen, AP = arboreal pollen). Arrows indicate the location of extreme floods (clay laminations in peaty matrix), squares represent AMS dates in radiocarbon ages (upper sample: SUERC-37131, *Alnus* twig and bud; lower sample: SUERC-37130, *Alnus* twig), and black circles mark the location of samples for the palynological analyses.

(scenario 5). Because the main aim was to obtain a minimum for the peak discharge value, the lower PSI level of 18.4 m +OD was adopted as the BGE.

Slopes

Channel and floodplain surface slopes of the various compartments were derived from locally collected geological borehole data and geomorphological analysis (Van Munster 2011). These were compared with more regional estimates by Erkens *et al.* (2011). In scenario 6, a range for the slope of each compartment was set up from these two information sources (Table 1). Differences in slope mainly originate from the distance over the research area that was used to calculate individual slopes. The slope of the channel compartment (Zone E; Figure 2) was corrected for thalweg sinuosity of palaeochannels. Based on the palaeogeographic reconstruction of the fluvial history of this region (Figure 3), the BGE for the sinuosity was 1.3 (present is ~1.2) with a maximum of 1.5 (scenario 7; Table 1). These estimates relate to the choice and likeliness of HG or SB for channel shape.

Examples from other palaeohydrological studies (the majority of which are from confined valleys using slackwater PSIs, or from tributaries rather than our floodplain PSIs) highlight that water slope deviations due to non-uniform flow contribute significantly to the uncertainty in discharge calculations (e.g., Webb & Jarrett 2002). A strongly schematic DEM of the Middle Holocene Lower Rhine Valley was used to assess the effect of water slope variations during non-uniform flow conditions. Non-uniform flow is mainly caused by the downstream variations in valley/floodplain width, and fluvial style. Test runs with the SOBEK 2D-hydraulic model (Delft Hydraulics and Dutch Ministry of Transport, Public Works and Water Management 1997) revealed local water level differences due to water slope effects to be 2 dm at maximum in our research area. Given the location of our PSIs on terraces flanking the channel, these water level deviations are minor compared to other effects influencing the calculated discharges. In our relatively wide and low gradient lower valley setting (with a rather uniform valley shape), 50 km upstream of the Middle Holocene delta apex, and ~180 km upstream of the coastline, the passage of extreme flood waves seems to be less affected by spatial effects and non-uniform flow effects than in the steep, confined settings of other studies. Further non-uniform flow effects were not evaluated in our modelled scenarios.

Roughness

Two types of surface roughness were distinguished: in channel bed roughness and vegetation roughness in floodplain areas. Bed roughness in channels can be predicted based on grain size ($k_s = 3{*}D_{90}$), dune heights ($k_s = 0.5{*}h_{\mathrm{dune}}$), or can be calibrated from velocity profile measurements of an observed discharge wave (Van Rijn 1984). In scenario 8, a range is set up for k_s (Table 1). To estimate k_s, data were used from bed form roughness studies in the Lower Rhine at the Dutch–German border (Kleinhans *et al*. 2011), located ~30 km downstream of our modelled cross-section. There, bed material and substrate geology are very similar to these at our transect location. The minimum discharge scenario uses a relatively high value for k_s that is based on dune heights (h_{dune}) in the thalweg of the Rhine at maximum discharges in 1995 and 1998 (Wilbers & ten Brinke 2003; Frings & Kleinhans 2008). The maximum discharge scenario uses a relatively low value based on an estimated D_{90} for Rhine thalweg sediment (Frings & Kleinhans 2008). The BGE is an intermediate value that is consistent with values based on velocity profiles of the 1995 flood and historical floods (Hesselink & Kleinhans 2002). The values are applied over the full width of the open channel segment, which locally causes an overestimate of k_s at the channel fringes. However, k_s values have been estimated from moderate floods; extreme floods likely form larger dunes with higher k_s values in the middle of the channel, thereby compensating for the underestimate at the channel fringes.

For each floodplain compartment (Zones A–D; Figure 2), vegetation roughness was taken as a single value. The vegetation generally consisted of riparian forest, which was dominated on the lower parts of the floodplain by dense *Salix* and *Alnus* stands of up to 6 m high; on the upper parts by *Quercus* and *Alnus*. It is unlikely that large strips of bare soil (or open grassland) existed on the floodplain prior to forest clearance and the beginning of agriculture (Figure 4). Vegetation roughness coefficients were calculated for every floodplain compartment (Table 2), based on bulk drag coefficients, vegetation density and the average size of tree stems (variable in scenario 10). A range in parameters was set up from information from vegetation guides (Wolf *et al*. 2001; Van Velzen *et al*. 2002a, 2002b) and is in agreement with observations in plots of currently unmanaged riparian vegetation, and information on the general vegetation composition from the pollen assemblages in the investigated abandoned channel fill (Figure 4). Scenario 9 was created to estimate the effect of vegetation composition ratios (different proportions of pioneer vegetation in stands of forest). This was only done for the floodplain compartment adjacent to the open channel, because this area is most influenced by fluvial erosion and deposition, which creates suitable locations for pioneer vegetation to establish. Moreover, this low-lying zone is submerged in deeper waters during floods than other floodplain compartments, so especially here, differences in vegetation composition may induce large variations in discharge.

At present, uncertainties in floodplain vegetation roughness estimates are up to ~30%, despite the use of modern techniques (Straatsma & Huthoff 2011). This leads to water

level deviations of several decimetres for a given discharge. As no detailed reference for specific natural floodplain vegetation exists, there is little merit in attempting an extremely data-demanding method for accurately reconstructing past vegetation. Instead, a wide range of vegetation densities and stem sizes was used to determine their effect on the total discharge (Table 1). Because vegetation parameters were assumed to be the same for various vegetation types on the different terraces (Van Velzen *et al.* 2002a), the palaeofloodplain vegetation was treated as a single forest type per zone in Figure 2. The range of different vegetation densities was represented by varying mean density values per floodplain compartment (Table 2).

Validation test with observed discharges

A validity check of the method and parameters used was performed on the DEM of the embanked floodplain for the gauged discharges of the 1993 and 1995 floods (at Rees; Figure 1). For this test, surface roughness of the grasslands in the present floodplain and modern channel depth profiles were adopted respectively from Van Velzen *et al.* (2002a) and Baur & Jagers (2002). With the BGE estimates (Table 1), modelled discharges were ~3% lower than the observed discharges (11,100 $m^3 s^{-1}$ in 1993; 11,800 $m^3 s^{-1}$ in 1995).

PALAEOFLOOD DISCHARGES

Palaeoflood magnitudes

The BGE discharge outcome is 13,250 $m^3 s^{-1}$ (Table 3). The outcomes of the various scenarios vary over a wide range (7,300–25,600 m^3 sec^{-1}) as a result of the broad range of possible values (Table 1). Plausibly, some input parameters may deviate from our BGE and could be near the values of the minimum and maximum for scenarios. It is, however, highly unlikely that all factors deviate in the same direction (towards lower or upper limits) and that such a combination results in a realistic estimate for the minimum magnitude of extreme palaeofloods in the Middle Holocene. The value of our BGE slightly exceeds the largest measured flood of AD 1926 (12,600 m^3 sec^{-1}), but is lower than the reconstructed magnitude of the AD 1374 flood. Herget & Meurs (2010) calculated the AD 1374 flood at Cologne to have peaked at 18,800 m^3 sec^{-1} (adopting their minimal scenario). A difficulty is that palaeochannel shape and urban surface roughness for medieval Cologne and surroundings are essentially unknown and harder to reconstruct than for the Middle Holocene situation of our study area. Modelling studies that link generated stochastic rainfall to catchment-scale discharge routing and valley-scale flood wave propagation models generate Q_{1250} floods of 16,700–18,500 $m^3 s^{-1}$ (Te Linde *et al.* 2010). Our BGE extreme palaeoflood is below these values, reflecting our conservative aim to provide a realistic geological *minimal* limit for extreme paleofloods. With the effects explored using the maximum parameter values in scenarios (Table 3), the Middle Holocene PSIs could match a similar flood magnitude as the ones reconstructed and simulated in previous studies. However, a present flood event with a similar recurrence interval as the Middle Holocene flood would probably generate a larger discharge, because deforestation has increased effective runoff in the catchment area and canalization and embankment have caused a steepening of the peak discharge wave (discussed below).

The lower limit of 7,300 $m^3 s^{-1}$ is strikingly low given that it is based on a PSI that is considered to be the result of a 'rare' and 'extreme' flood. Floods of this magnitude are estimated to recur every ~5 years in the Lower Rhine at present (Chbab *et al.* 2006). Accepting this lowest value as an extreme flood would imply that the Middle Holocene discharge regime was very different from the last century and historic times. The outcome is mainly this low because of the assumed channel dimensions (paleochannel SB in scenario 4; −30% effect). The lower limit for scenarios adopting HG for channel shape is ~10,500 $m^3 s^{-1}$, and these are the morphological scenarios that fit the palaeogeographical setting more logically.

The maximum modelled outcome is 25,600 $m^3 s^{-1}$. This represents an unlikely theoretical maximum for the value of the lower limit of extreme palaeofloods in the Middle Holocene, as it was obtained for the parameter combination that pushes all factors to the maximum discharge producing values that are thought to be possible. It includes a maximum water surface elevation of 1.1 m above PSIs valley-wide. Current flood frequency extrapolation estimates (Chbab *et al.* 2006) suggest such palaeoflows to occur more rarely than once in 10,000 years. In the context of

Table 3 | Modelled discharges for palaeofloods in the Middle Holocene Lower Rhine (BGE, MIN, MAX), and deviations compared to BGE per varying model parameter

		Discharge m^3/s			
Best guess estimate		13,244			
Overall minimum		7,328			
Overall maximum		25,594			
Individual scenarios					
Input	**Scenario**	**MIN**	**%**	**MAX**	**%**
Hydraulic total		*8,721*	*− 34%*	*18,070*	*+ 36%*
1	Lange Renne bypass	BGE	–	13,373	+1%
2	EH overbank	BGE	–	13,360	+1%
3	LH sedimentation	12,573	−5%	14,393	+9%
4	Palaeochannels	9,264	−30%	BGE	–
5	PSIs	BGE	–	16,497	+25%
Slope total		*12,054*	*−9%*	*15,401*	*+16%*
6	Floodplain slopes	12,869	−2%	14,801	+12%
7	Channel sinuosity	12,428	−6%	13,727	+4%
Roughness total		*12,224*	*−8%*	*15,996*	*+21%*
8	Bed roughness	12,249	−8%	14,594	+10%
9	Vegetation ratio	13,192	−0%	13,453	+2%
10	Vegetation density	BGE	–	14,403	+9%

flood safety measures at regional scale, design focuses on rare events (such as Q_{1250}) but not on freak events; floods that are generated by other mechanisms than normal meteorologically induced floods and occur far beyond that range. Figures on freak events may be important for local protection (e.g., nuclear power plants), but would be prohibitively costly to apply regionally.

Recurrence interval

In the period covered by the PSI-containing channel fill, only two extreme flood events were registered in the period 7.8–4.1 ka BP (AMS dates and pollen data in Figure 4). The position high above the channel system of the same age is reason to consider them deposits from rare magnitude events. Only the upper event layer is modelled, as it probably represents a larger event with higher water levels than the lower PSI of the earlier event – although the limited difference of ~0.2 m would probably not produce significantly different results. The position of the event layers within the dated interval suggests a recurrence interval between 1,250 and 2,500 years; there are only two events in the dated interval of ~5,000 (calendar) years, but because both layers are located in the later half of this period, a minimum recurrence interval of 1,250 years was adopted.

This range for recurrence intervals only applies to the flooding regime in the dated interval (Figure 4). It is possible that non-stationarity in the flooding regime complicates utilization of these observations in the assessment of recurrence intervals of extreme floods at present (Redmond *et al.* 2002; Milly *et al.* 2008). Even though no major differences in climate exist between the Middle Holocene and the last centuries for the research area (Davies *et al.* 2003), minor climatic changes may have influenced recurrence intervals of floods (Knox 1993), and caused the occurrence of intensified flooding episodes (Macklin *et al.* 2006). However, the effect of non-stationarity on extreme events, which approach the physical limit of meteorologically induced flood magnitudes, is largely unexplored scientific terrain. Therefore, it may well be that the

effect of climatic-induced non-stationarity is *not* sufficient to significantly affect recurrence intervals in the range of extreme floods.

Effect of parameter uncertainty

In the case of this study, palaeotopography, slope and roughness turn out to contribute significantly to total uncertainty (Table 3). The combined effects of these parameter groups are at least an 8% deviation from the total BGE discharge. A further breakdown of introduced uncertainty shows that channel geometry, flood levels (PSIs), slopes and bed roughness are the main contributors, with each a >10% effect on the total discharge. Although channel geometry and the PSIs are precisely reconstructed in the field, still the estimated parameter ranges are relatively wide (Table 1). Slopes have also been reconstructed accurately and the range is rather limited, but still the induced uncertainty is large. This indicates that small variations in slope have a major influence on modelled discharges.

Smaller individual contributions (<5% effect) to the uncertainty in modelled discharge result from the stripping of Late Holocene overbanks on higher terrace levels, adjusting anthropogenic by-pass channels, and varying vegetation composition on the lower part of the Middle Holocene floodplain. In the case of the Late Holocene overbanks, it is clear that this is caused by the tight range of the input data. The minor effect of the anthropogenic by-pass channel can be ascribed to its limited size and location on a relatively high terrace level. No large water depths are reached even during an extreme flood. The effect of vegetation ratios and vegetation in general is more difficult to assess. It was thought that the vegetation would have a profound effect on modelled discharges and uncertainty – even more when the low accuracy and wide range of set-up model parameters are considered (Table 2). A possible explanation is that flow velocities are, compared to slope-induced variations, relatively insensitive to vegetation roughness. Perhaps a larger effect can be forced with a wider range of vegetation types and densities, especially when a dominance of grass- and shrublands are considered to be possible in the Middle Holocene floodplains of the Lower Rhine. So far, palynological information gives, however, no reason to adopt such scenarios in the investigated period, as the pollen spectra are dominated by arboreal species (Figure 4).

IMPLICATIONS FOR FUTURE FLOOD PREDICTIONS

To use the minimal magnitude of Middle Holocene palaeoflood extremes in flood frequency analysis for the *present* situation, issues regarding the translation of the past to the modern catchment run-off situation and flood-wave dynamics need to be addressed. Non-stationarity in palaeohydrology is often thought to be primarily produced by natural climatic variations, but in the setting of the Middle and Late Holocene Rhine (pre)historic human actions may have had stronger progressive effects on the river and its flooding regime (Erkens *et al.* 2006; Hoffmann *et al.* 2007). To allow projection of our results to the present, human-induced changes need to be assessed on a catchment scale. Deforestation became significant at catchment scale in the Bronze Age (i.e., since ~3.5 ka BP). The increasing sediment supply and effective run-off by a decrease in the buffering effect of vegetation may have resulted in more discharge to be released from catchments under similar meteorological conditions. Hundecha & Bárdossy (2004) indicated that a given amount of precipitation results in 10–19% higher peak discharges nowadays than in a fully forested catchment for magnitudes of the 1993/1995 floods in major tributaries of the Rhine. Ward *et al.* (2011) report corresponding results for similar floods in the Meuse catchment. Importantly, the effect of deforestation on Q_{1250} appears to be non-significant in their model, in contrast to the effect on moderate events.

In addition, major engineering works have been carried out on the Rhine: the river has been embanked and straightened in recent centuries. This effectively reduced river length and eased the downstream transport of large discharge volumes (Disse & Engel 2001). It enabled the same volume of water to pass in less time, which causes higher peak discharges and higher peak water levels by a steepening of discharge waves (Lammersen *et al.* 2002). The impact of this effect on Q_{1250} is estimated as 6% since the beginning of the Industrial Revolution (Parmet *et al.* 2001; Lammersen *et al.* 2002). Recent river and floodplain adjustments, focusing on the construction of retention basins, are expected to flatten the discharge wave again (Lammersen *et al.* 2002).

Although more specific research is needed on the actual effect of the above discussed factors, especially for extreme floods, the combined effect on discharge of these major changes for the Lower Rhine is conservatively estimated to range between 6 and 16% since human impact began. In this combined estimate, the effect of river training is considered minor (Lammersen *et al.* 2002) compared to the possible effect of deforestation (Hundecha & Bárdossy 2004). As indicated by Ward *et al.* (2011), the effect of deforestation on extreme floods may be smaller than the effect on large floods (similar to the 1993/1995 floods), so the lower estimate of 10% change by deforestation by Hundecha & Bárdossy (2004) was adopted. Accordingly, our BGE for Middle Holocene extreme floods would correspond to a discharge that ranges between 14,050 and 15,370 $m^3 s^{-1}$ under modern conditions; discharges that have not been observed in the last century, but are very close to the present design standard.

In frequency-magnitude plots, the range of modelled palaeodischarge outcomes presents a lower limit of possible palaeoflood magnitudes. Figure 5 plots our BGE plus 6–16% 'deforestation and engineering' with a recurrence interval of 1,250 to 2,500 years. This lower limit for flood magnitude and the range in recurrence interval provide a geological check for the current Q_{1250} in the Lower Rhine. The current frequency-magnitude relation (Chbab *et al.* 2006) corresponds well to our lower limit for extreme events. Because this study is not suitable for producing an accurate estimate for the upper limit of palaeoflood discharges, no conclusions can be drawn regarding the maximum discharge values and the upper range of uncertainties in current estimates of flood frequency analysis.

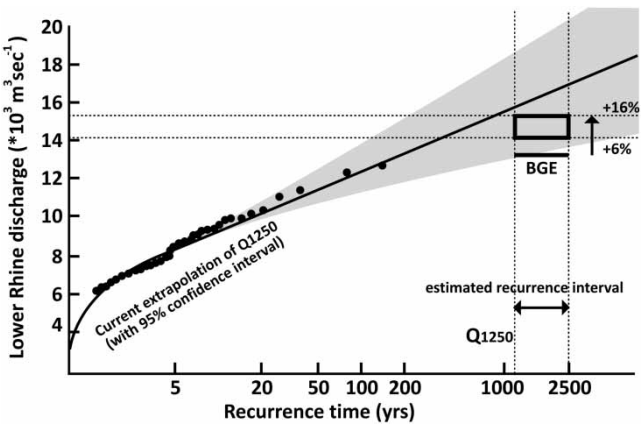

Figure 5 | Current flood magnitude-frequency extrapolation (redrawn after Chbab *et al.* 2006) with our calculated range in recurrence interval and the BGE for the lower limit of Middle Holocene palaeoflood extremes. The BGE is corrected with +6 to 16% for 'deforestation and engineering' – see main text.

To further exploit Middle Holocene paleoflood results and to make it an effective way to reduce uncertainty in flood frequency analysis, uncertainty in the magnitude estimates should be narrowed further. This can be done by: (1) carrying out a similar exercise at alternative suitable transect locations in the Lower Rhine Valley – for example at the present day delta apex; (2) improving accuracy of input parameters; and (3) assessing the effect of major changes in the catchment on Q_{1250} using numerical modelling for palaeosituations. In the case of non-stationarity it is important to accurately quantify the differences in discharges for similar extreme floods in terms of generated runoff and recurrence intervals between different periods during the last 5,000 years.

In spite of the uncertainty in the reconstructed peak discharges of palaeofloods, millennial-scale geological evidence is extremely useful for estimating modern flood safety limits. Modern gauged records are too short for predicting extreme events, while historical records are mostly inaccurate and need additional reconstruction techniques to estimate flood magnitudes. Geological records provide a unique resource for the reconstruction of extreme events and are particularly useful in obtaining physical limits for flood magnitudes despite the associated uncertainty. For the Late Holocene, there is even more geological evidence available from palaeochannel fills and floodplains, which can be used for palaeohydrological modelling, also for less rare events. Further research should aim at predicting the frequency and magnitude of large flooding events from these records to verify and further constrain the results from this study. Further integration of historical and palaeofloods with modern floods is also essential, so that the design standard for dikes is established more accurately.

CONCLUSIONS

A Chézy-based hydraulic model, using a slope–area approach, was run to estimate the magnitude of extreme floods of the Middle Holocene age in the Lower Rhine

Valley. For such extreme events, dating to between 4.1 and 7.9 ka BP, palaeostage indicators have registered in a filling palaeochannel located on a relatively high floodplain terrace. Ten explorative scenarios regarding the sensitivity to various input parameters, based on geological, geomorphological and vegetation information, give a best guess range estimate for the size of the minimal exceeded discharge during the PSI-producing events. The resulting best guess estimate modelled discharge is 13,250 $m^3 sec^{-1}$, which exceeds gauged floods of the last century. The recurrence interval of floods exceeding this value is estimated to be between 1,250 and 2,500 years.

The sensitivity analysis shows that besides the exact flood level, the palaeochannel geometry, slope reconstructions and bed roughness estimates are the main contributors to uncertainty in discharge estimates. For most input parameters this is a direct effect of a relative wide range of possible values, despite the accurate reconstruction of associated physical limits in the palaeolandscape. Modelled discharges are particularly sensitive to bed slope estimates, which are defined in a narrow range, but still introduce a significant amount of uncertainty in model outcomes.

For application in modern flood frequency analysis, palaeodischarge results must be converted to equivalent discharges for the modern situation with altered hinterland land cover and embanked and straightened rivers. Applying literature-based conversions suggests a 6–16% increase in absolute discharge. This suggests that our BGE coincides with the currently used design flood in the Lower Rhine Valley.

ACKNOWLEDGEMENTS

We acknowledge Utrecht University MSc students A. Geurts and B. van Munster for participating in the fieldwork. We thank W. Z. Hoek, G. Erkens and K. M. Cohen (Utrecht University) for field assistance. K. M. Cohen, W. I. van de Lageweg and M. G. Kleinhans (Utrecht University), and two anonymous reviewers are thanked for comments on earlier versions of the manuscript and model. Neil Macdonald (University of Liverpool) and Jürgen Herget (Bonn University) are thanked for organizing and editing this special issue on 'Palaeofloods in Earth's History'. This research was funded by Deltares, with additional funding from TNO Geological Survey of The Netherlands, and Utrecht University.

REFERENCES

Baker, V. R. 1987 Paleoflood hydrology and extraordinary flood events. *J. Hydrol.* **96**, 79–99.

Baker, V. R., Webb, R. H. & House, P. K. 2002 The scientific and societal value of paleoflood hydrology. In: *Ancient Floods, Modern Hazards: Principles and Applications of Palaeoflood Hydrology* (P. K. House, R. H. Webb, V. R. Baker & D. Levish, eds). Water Science and Application 5, American Geophysical Union, pp. 1–19.

Baptist, M. J., Babovic, V., Uthurburu, J. R., Keijzer, M., Uittenbogaard, R. E., Mynett, A. & Verwey, A. 2007 On inducing equations for vegetation resistance. *J. Hydraul. Res.* **45** (4), 435–450.

Baur, T. & Jagers, H. R. A. 2002 Grensproject Bovenrijn/ Grenzprojekt Niederrhein, Model construction, calibration and verification. Report Q2496.00, WL-Delft Hydraulics, Delft.

Benito, G., Lang, M., Barriendos, M., Llasat, M. C., Frances, F., Ouarda, T., Thorndycraft, V. R., Enzel, Y., Bardossy, A., Coeur, D. & Bobee, B. 2004 Use of systematic, palaeoflood and historical data for the improvement of flood risk estimation. Review of scientific methods. *Nat. Hazards* **31**, 623–643.

Chbab, E. H. 1996 How extreme were the 1995 flood waves on the Rivers Rhine and Meuse? *Phys. Chem. Earth* **20**, 455–458.

Chbab, E. H., Buitenveld, H. & Diermanse, F. 2006 Estimating exceedance frequencies of extreme river discharge using statistical methods and physically based approach. *Osterr. Wasser- Abfallwirtsch.* **58**, 35–43.

Cohen, K. M., Stouthamer, E., Hoek, W. Z., Berendsen, H. J. A. & Kempen, H. F. J. 2009 *Zand in banen (3e druk). Sand-depth maps of the central and upper Rhine-Meuse delta, including the IJssel valley (with summary in English)*. Universiteit Utrecht/Provincie Gelderland, Utrecht, The Netherlands. 75 pp.+ CD-ROM.

Dalrymple, T. & Benson, M. A. 1968 Measurement of peak discharge by the slope-area method. U.S. Geological Survey Techniques in Water Resources Investigations 3:A2, 12. Available from: http://pubs.usgs.gov/twri/twri3-a2/.

Davies, B. A. S., Brewer, S., Stevenson, A. C., Guiot, J., Data Contributors. 2003 The temperature of Europe during the Holocene reconstructed from pollen data. *Quaternary Sci. Rev.* **22**, 1701–1716.

Delft Hydraulics and Dutch Ministry of Transport, Public Works and Water Management 1997 SOBEK, Technical Reference Manual.

Disse, M. & Engel, H. 2001 Flood events is the Rhine Basin: Genesis, influences and mitigation. *Nat. Hazards* **23**, 271–290.

Erkens, G., Cohen, K. M., Gouw, M. J. P., Middelkoop, H. & Hoek, W. Z. 2006 Holocene sediment budgets of the Rhine Delta (The Netherlands): a record of changing sediment delivery. *IAHS-AISH P* **306**, 406–415.

Erkens, G., Hoffmann, T., Gerlach, R. & Klostermann, J. 2011 Complex fluvial response to Lateglacial and Holocene allogenic forcing in the Lower Rhine Valley (Germany). *Quaternary Sci. Rev.* **30** (5–6), 611–627.

Frings, R. M. & Kleinhans, M. G. 2008 Complex variations in sediment transport at three large river bifurcations during discharge waves in the river Rhine. *Sedimentology* **55**, 1145–1171.

Geurts, A. 2011 Weichselian to Early Holocene vegetation development and fluvial adjustment in the Lower Rhine Valley, Germany. Unpublished MSc thesis, Department of Physical Geography, Utrecht University, Utrecht, The Netherlands.

Herget, J. & Euler, T. 2010 Hoch- und Niedrigwasser in historischer und prähistorischer Zeit. *Geographische Rundschau* **62** (3), 4–10.

Herget, J. & Meurs, H. 2010 Reconstructing peak discharge for historic flood levels in the city of Cologne, Germany. *Glob. Planet. Change* **70**, 108–116.

Herget, J., Euler, T., Roggenkamp, T. & Zemke, J. 2013 Obstacle marks as palaeohydraulic indicators of Pleistocene megafloods. *Hydrol. Res* **44** (2), 300–317.

Hesselink, A. W. & Kleinhans, M. G. 2002 Channel pattern and flow characteristics of the Rhine distributaries in historic time, The Netherlands. In: Hesselink, A.W. History makes a river, PhD dissertation, Utrecht University, Utrecht, The Netherlands.

Hoffmann, T., Erkens, G., Cohen, K. M., Houben, P., Seidel, J. & Dikau, R. 2007 Holocene floodplain sediment storage and hillslope erosion within the Rhine catchment. *Holocene* **17**, 105–118.

Hundecha, Y. & Bárdossy, A. 2004 Modeling of the effect of land use changes on the runoff generation of a river basin through parameter regionalization of a watershed model. *J. Hydrol.* **292**, 281–295.

Keijzer, M., Babovic, V., Bastist, M. & Uthurburu, J. R. 2005 Determining equations for vegetation induced resistance using genetic programming. *Conference Proceeding GECCO 2005 – Genetic and Evolutionary Computation Conference*, Washington, DC, June 2005.

Keulegan, G. H. 1938 Laws of turbulent flow in open channels. *J. Res. Nat Bur. Stand.* **21**, 707–741.

Kleinhans, M. G., Cohen, K. M., Hoekstra, J. & IJmker, J. M. 2011 Evolution of a bifurcation in a meandering river with adjustable channel widths, Rhine delta apex, The Netherlands. *Earth Surf. Proc. Land.* **36**, 2011–2027.

Klostermann, J. 1992 *Das Quartär der Niederrheinischen Bucht – Ablagerungen der letzten Eiszeit am Niederrhein*. Geologisches Landesamt Nordrhein-West-falen, Krefeld.

Knox, J. C. 1993 Large increases in flood magnitude in response to modest changes in climate. *Nature* **361**, 430–432.

Kwadijk, J. C. J. & Middelkoop, H. 1994 Estimation of impact of climate change on the peak discharge probability of the River Rhine. *Clim. Change* **27**, 199–224.

Lammersen, R., Engel, H., van de Langemheen, W. & Buiteveld, H. 2002 Impact of river training and retention measures on flood peaks along the Rhine. *J. Hydrol.* **267**, 115–124.

Lang, A., Bork, H. R., Mäckel, R., Preston, N., Wunderlich, J. & Dikau, R. 2003 Changes in sediment flux and storage within a fluvial system: some examples from the Rhine catchment. *Hydrol. Process.* **17**, 3321–3334.

Lechner, A. 2009 Palaeohydrologic conditions and geomorphic processes during the Postglacial in the Palatine Upper Rhine river floodplain. *Z. Geomorphol.* **53** (2), 217–245.

Levish, D. R. 2002 Paleohydrologic bounds: non-exceedance information for flood hazard assessment. In: *Ancient Floods, Modern Hazards: Principles and Applications of Paleoflood Hydrology* (P. K. House, R. H. Webb, V. R. Baker & D. R. Levish, eds). Water Science and Application 5, American Geophysical Union, Washington, DC, pp. 175–190.

Macklin, M. G., Benito, G., Gregory, K. J., Johnstone, E., Lewin, J., Michczynska, D. J., Soja, R., Starkel, L. & Thorndycraft, V. R. 2006 Past hydrological events reflected in the Holocene fluvial record of Europe. *Catena* **66**, 145–154.

Milly, P. C. D., Betancourt, J., Falkenmark, M., Robert, M., Hirsch, R. M., Kundzewicz, Z. W., Lettenmaier, D. P. & Stouffer, R. J. 2008 Stationarity is dead: Whither water management? *Science* **319**, 573–574.

O'Connell, D. R. H., Ostenaa, D. A., Levish, D. R. & Klinger, R.E. 2002 Bayesian flood frequency analysis with paleohydrologic bound data. *Water Resour. Res.* **38**, 16.1–16.13.

Parmet, B. W. A. H., van de Langemheen, W., Chbab, E. H., Kwadijk, J. C. J., Diermanse, F. L. M. & Klopstra, D. 2001 Analyse van de maatgevende afvoer van de Rijn te Lobith. Rijkswaterstaat, Arhnem, RIZA rapport 2002.012.

Redmond, K. T., Enzel, Y., House, P. K. & Biondi, F. 2002 Climate impact on flood frequency at the decadal to millennial time scales. In: *Ancient Floods, Modern Hazards: Principles and Applications of Palaeoflood Hydrology* (P. K. House, R. H. Webb, V. R. Baker & D. Levish, eds). Water Science and Application 5, American Geophysical Union, pp. 21–45.

Shabalova, M. V., van Deursen, W. P. A. & Buishand, T. A. 2003 Assessing future discharge of the river Rhine using regional climate model integrations and a hydrological model. *Climate Res.* **23**, 233–246.

Straatsma, M. & Huthoff, F. 2011 Uncertainty in 2D hydrodynamic models from errors in roughness parameterization based on aerial images. *Phys. Chem. Earth* **36**, 324–334.

Te Linde, A. H., Aerts, J. C. J. H., Bakker, A. M. R. & Kwadijk, J. C. J. 2010 Simulating low-probability peak discharges for the Rhine basin using resampled climate modeling data. *Water Resour. Res.* **46**, W03512.

Toonen, W. H. J., Kleinhans, M. G. & Cohen, K. M. 2012 Sedimentary architecture of abandoned channel fills. *Earth Surf. Proc. Land.* **37**, 459–472.

Van Munster, B. 2011 Early and Middle Holocene fluvial development near the present-day Rhine Delta apex, Germany. Unpublished MSc thesis, Department of Physical Geography, Utrecht University, Utrecht, The Netherlands.

Van Rijn, L. C. 1984 Sediment transport, part III: bed forms and alluvial roughness. *J. Hydraul. Eng.* **110** (12), 1733–1754.

Van Velzen, E. H., Jesse, P., Cornelissen, P. & Coops, H. 2002a Stromingsweerstand vegetatie in uiterwaarden, Deel 1 handboek versie 1.0. Rijkswaterstaat, Directie Oost Nederland, RIZA werkdocument 2002.140x.

Van Velzen, E. H., Jesse, P., Cornelissen, P. & Coops, H. 2002b Stromingsweerstand vegetatie in uiterwaarden, Deel 2 achtergronddocument versie 1.0. Rijkswaterstaat, Directie Oost Nederland, RIZA werkdocument 2002.141x.

Ward, P. J., Renssen, H., Aerts, J. C. J. H. & Verburg, P. H. 2011 Sensitivity of discharge and flood frequency to twenty-first century and late Holocene changes in climate and land use (River Meuse, northwest Europe). *Clim. Change* **106**, 179–202.

Webb, R. H. & Jarrett, R. D. 2002 One-dimensional estimation techniques for discharges of paleofloods and historical floods. In: *Ancient Floods, Modern Hazards: Principles and Applications of Palaeoflood Hydrology* (P. K. House, R. H. Webb, V. R. Baker & D. Levish, eds). Water Science and Application 5, American Geophysical Union, pp. 111–125.

Wilbers, A. W. E. & ten Brinke, W. B. M. 2003 The response of subaqueous dunes to floods in sand and gravel bed reaches of the Dutch Rhine. *Sedimentology* **50**, 1013–1034.

Wolf, R. J. A. M., Stortelder, A. H. F. & de Waal, R. W. 2001 *Ooibossen. Bosecosystemen van Nederland*. KNNV Uitgeverij, Utrecht.

First received 4 November 2011; accepted in revised form 6 July 2012. Available online 12 November 2012